Article
Chinese Science Bulletin
SPECIAL ISSUE: New Energy Materials
November 2012 Vol.57 No.32: 4233–4236
doi: 10.1007/s11434-012-5072-8

Pure water splitting to generate H_2 over strontium niobate and tantalate: A comparative study

LIANG ShiJing, SHEN LiJuan & WU Ling*

State Key Laboratory of Breeding Base of Photocatalysis, Fuzhou University, Fuzhou 350002, China

Received November 15, 2011; accepted January 17, 2012; published online March 31, 2012

To clarify the nature of different photocatalytic activities between niobate and tantalate, a comparative study of the water splitting into H_2 over strontium niobate and tantalate was performed. These isostructural photocatalysts were prepared by a facile and simple hydrothermal reaction and characterized by powder X-ray diffraction (XRD), N_2-sorption, UV-Vis diffuse reflectance spectra (UV-Vis DRS), and transmission electron microscopy (TEM). The effects of crystal structure, Brunauer-Emmett-Teller (BET) surface area, photoabsorption performance, morphology, and electronic structure are discussed.

niobate, tantalate, water splitting, photocatalysis, comparative study

Citation: Liang S J, Shen L J, Wu L. Pure water splitting to generate H_2 over strontium niobate and tantalate: A comparative study. Chin Sci Bull, 2012, 57: 4233–4236, doi: 10.1007/s11434-012-5072-8

Photocatalytic water splitting is an ideal route for hydrogen production, and has been intensively studied as an environmentally safe solution to the energy problem [1,2]. Since the layered $K_4Nb_6O_{17}$ was reported [3], numerous studies have been carried out on niobate and tantalate photocatalysts due to their unique structure and high performance in photocatalytic reactions [4,5]. Particularly, in terms of quantum efficiency (QE), the record holder is NiO/$NaTaO_3$:La, with a QE of 56% for water splitting [6]. Although photocatalytic water splitting over niobate and tantalate catalysts has been widely investigated, previous studies have mainly focused on development of synthetic methods for preparation of new catalysts. Photocatalytic activity comparisons between isostructural niobate and tantalate are rare. In this work, we investigate the activity of strontium niobate and tantalate photocatalysts prepared by our recently-developed methods [7–9]. Discussions of the photocatalytic activity are based on differences in crystal structure, BET surface area, photoabsorption performance, electronic structure, and morphology of the catalytic materials.

1 Experimental

Isostructural strontium niobate ($Sr_{0.4}H_{1.2}Nb_2O_6{\cdot}H_2O$) and tantalate ($Sr_{0.25}H_{1.5}Ta_2O_6{\cdot}H_2O$) nanopolyhedra photocatalysts were prepared from $Nb_2O_5{\cdot}nH_2O$ and $Ta_2O_5{\cdot}nH_2O$ as precursors, respectively, by a simple hydrothermal process, which is described in our previous reports [7–9]. Briefly, a mixture of the as-obtained $Nb_2O_5{\cdot}nH_2O$ [7] (or $Ta_2O_5{\cdot}nH_2O$ [8]) and $Sr(NO_3)_2$ in a molar ratio of Nb^{5+} (or Ta^{5+}):Sr^{2+} = 2:1 was dispersed in 70 mL deionized water. Then, the dispersion was adjusted to pH 10 with 4 mol L^{-1} NaOH under vigorous stirring. The resultant mixture was transferred to a Teflon-lined stainless steel autoclave. The autoclave was sealed and heated in an oven at 160°C for 24 h under autogenous pressure. After cooling, the products were centrifuged, washed with deionized water, and oven-dried at 60°C. Henceforth, we denote $Sr_{0.4}H_{1.2}Nb_2O_6{\cdot}H_2O$ and $Sr_{0.25}H_{1.5}Ta_2O_6{\cdot}H_2O$ as HSN and HST, respectively.

The as-prepared samples were characterized by powder X-ray diffraction (XRD) on a Bruker D8 Advance X-ray diffractometer operated at 40 kV and 40 mA with Ni-filtered Cu Kα irradiation (λ=1.5406 Å). The Brunauer-Emmett-Teller (BET) surface area was measured with an

*Corresponding author (email: wuling@fzu.edu.cn)

ASAP2020M apparatus (Micromeritics Instrument Corp.). Transmission electron microscopy (TEM) images were recorded using a JEOL model JEM 2010 EX microscope at an accelerating voltage of 200 kV. UV-Vis diffuse reflectance spectra (UV-Vis DRS) were obtained using a UV-Vis spectrophotometer (Varian Cary 500) and the data were converted to Kubelka-Munk (KM) functions. Barium sulfate was used as a reference.

The photocatalytic splitting reaction of pure water was performed in a closed gas-recirculation system and an inner irradiation quartz reaction cell with a 125 W high-pressure Hg lamp (the lamp intensity at 254 nm was 2.0 mW cm^{-2}; the distance between the lamp and the sensor was 1 cm). The reaction was carried out in pure water (50 mg catalyst, 170 mL H_2O). The amount of H_2 evolved was analyzed with an in-line gas chromatograph (GC112A, Shanghai Precision Scientific Instrument Co, Ltd, TCD, N_2 carrier).

2 Results and discussion

Figure 1 shows the same crystal structure of $Sr_{0.4}H_{1.2}Nb_2O_6{\cdot}H_2O$ and $Sr_{0.25}H_{1.5}Ta_2O_6{\cdot}H_2O$. Their three-dimensional framework is built with corner-shared octahedral NbO_6 (TaO_6) units. In a NbO_6 (TaO_6) unit, the metallic atom is surrounded by six oxygen atoms placed at the vertices of an octahedron. The Sr atom, surrounded by eight oxygen atoms, is located in the cavity constructed by NbO_6 (TaO_6) units. There are two unique crystallographic O atoms: one bonded to Nb (Ta) and the other belonging to crystal water or dodecahedral SrO_8 units in the cavities. As shown in Figure 2, the XRD patterns of the as-prepared samples match well with cubic phase $Sr_{0.4}H_{1.2}Nb_2O_6{\cdot}H_2O$ (JCPDS: 77-1165) and $Sr_{0.25}H_{1.5}Ta_2O_6{\cdot}H_2O$ (JCPDS: 77-1170). No signatures for other crystalline by-products are found within the patterns, indicating that the products may be pure HSN and HST. The average crystallite sizes for the samples calculated using the Scherrer equation are ~40 nm. The BET-determined specific surface areas of HSN and HST are 51.4 and 34.9 $m^2\ g^{-1}$, respectively.

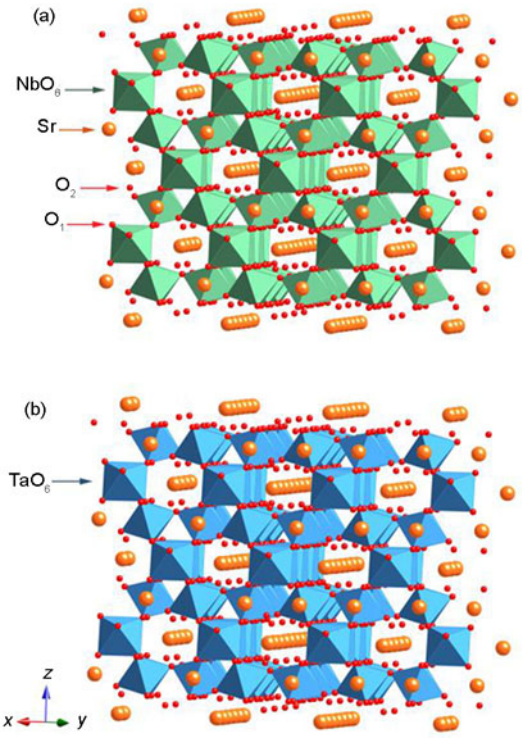

Figure 1 Schematic structure of strontium niobate and tantalite. (a) $Sr_{0.4}H_{1.2}Nb_2O_6{\cdot}H_2O$, (b) $Sr_{0.25}H_{1.5}Ta_2O_6{\cdot}H_2O$.

The optical absorption properties of HSN, HST, and TiO_2 (Degussa P25) samples have been characterized by UV-Vis DRS (Figure 3(a)). All the samples show strong absorption in the UV region, with absorption edges located at about 300, 254, and 387 nm, respectively. The absorption edge locations indicate that the redox ability of photogenerated charge carriers follows the order of HST > HSN > TiO_2. Because HSN and HST are isostructural, the valence bands of HSN and HST are mainly derived from the O 2p orbitals. The bandgap difference is caused by the different conduction band components. Figure 3(b) shows the band structure of HSN, HST, and TiO_2. The conduction level of HSN is similar to that of TiO_2 and about 0.7 eV lower than that of HST. All of them are higher than E^0 (H^+/H_2), indicating that the samples thermodynamically enable photocatalytic water splitting into H_2.

The morphologies of HSN and HST samples are characterized by TEM. Figure 4(a) shows that the HSN sample consisted of nanopolyhedra ranging from 40 to 70 nm and is well-dispersed. Similar nanopolyhedra can also be observed in the HST sample (Figure 4(c)). As shown in HRTEM images (Figure 4(b)), clear lattice fringes can be observed. The inter-planar spacing is consistent with the *d*-spacing of the corresponding lattice plane. The d = 0.61 nm fringes match the (111) crystallographic plane of cubic $Sr_{0.25}H_{1.5}Ta_2O_6{\cdot}H_2O$.

Figure 5 shows the photocatalytic activities for water

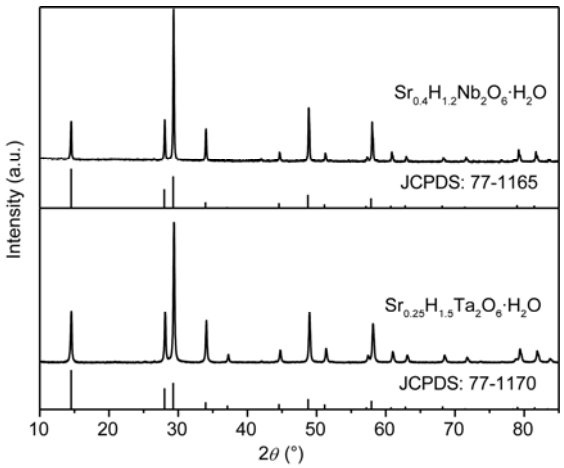

Figure 2 XRD patterns of HSN and HST.

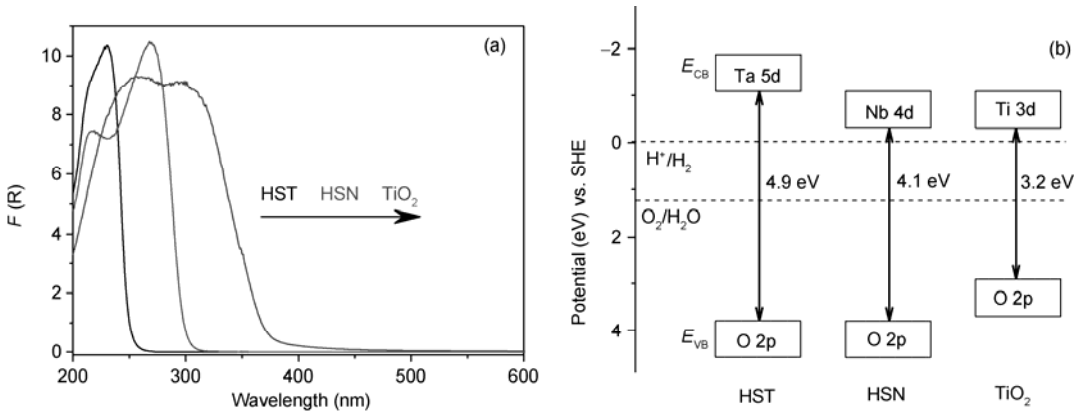

Figure 3 UV-Vis DRS (a) and band structure (b) of HSN, HST, and TiO_2.

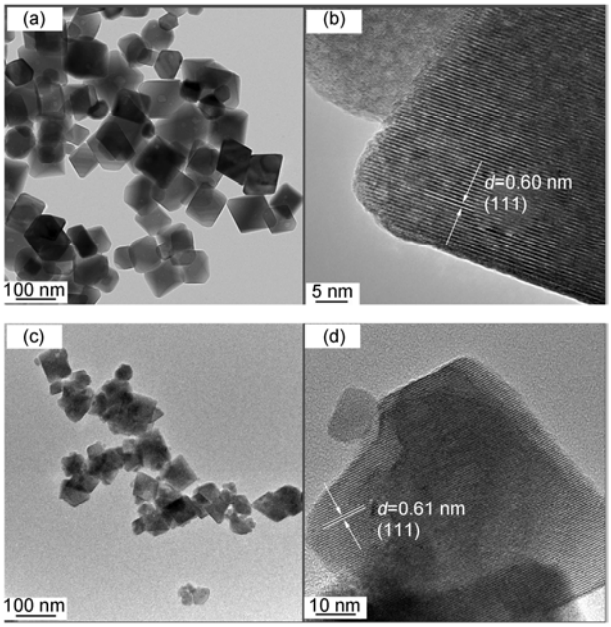

Figure 4 TEM (a, c) and HRTEM (b, d) images of HSN (a, b) and HST (c, d) samples prepared by reaction at 160°C at pH 10.

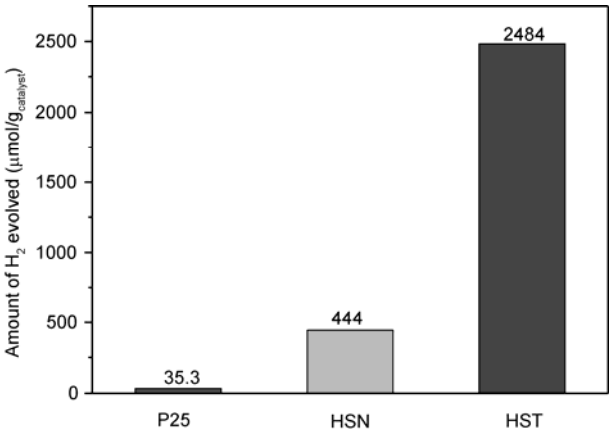

Figure 5 Photocatalytic activity of HSN, HST and TiO_2 with no co-catalyst.

splitting into H_2 over HSN, HST, and TiO_2 with no co-catalyst. The highest activity is obtained with the HST sample, which shows H_2 evolution of 2484 μmol/$g_{catalyst}$ after 6 h. This value is much higher than that of HSN (444 μmol/$g_{catalyst}$) and TiO_2 (35.3 μmol/$g_{catalyst}$). Since the number of absorbed photons for HST should be smaller than that of HSN and TiO_2 under the same experimental conditions, and the specific surface areas of HSN and P25 (TiO_2) are much higher than that of HST, the higher photocatalytic activity observed for HST may be attributed to other reasons. Because the HSN and HST samples have the same morphology and crystal structure, it may be concluded that the difference in electronic structure is the main factor for the different photocatalytic activities. That photogenerated electrons in HST have the highest reduction ability of the three samples may be one reason for its superior H_2 evolution rate. The other reason may be that the HST Ta 5d conduction band exhibits larger electron mobility when compared with the Nb 4d HSN conduction band.

3 Conclusion

Isostructural strontium niobate and tantalate nanopolyhedra photocatalysts were successfully prepared by a facile and simple hydrothermal reaction. For pure water splitting into H_2, the tantalate exhibits the highest photocatalytic activity compared with niobate and TiO_2. The superior catalytic activity may be attributed to the high reduction ability of its photogenerated electron and the high electron mobility of its conduction band. Differences in photoabsorption performance and BET surface area between the niobate and tantalite materials appear to have a negligible effect.

This work was supported by the National Natural Science Foundation of China (21177024), the Natural Science Foundation of Fujian Province (2011J01041), and the Program for Changjiang Scholars and Innovative Research Team in University (PCSIRT0818).

1 Gupta S M, Manoj T. A review of TiO_2 nanoparticles. Chin Sci Bull,

2011, 56: 1639–1657
2 Zhu Y, He Y, Wang R, et al. Albumin/zinc porphyrin conjugates for photosensitized reduction of water to hydrogen (in Chinese). Chin Sci Bull (Chin Ver), 2011, 56: 1360–1366
3 Domen K, Kudo A, Shibata M, et al. Novel photocatalysts, ion-exchanged $K_4Nb_6O_{17}$, with a layer structure. J Chem Soc Chem Commun, 1986, 1706–1707
4 Chen X, Shen S, Guo L, et al. Semiconductor-based photocatalytic hydrogen generation. Chem Rev, 2010, 110: 6503–6570
5 Kudo A, Miseki Y. Heterogeneous photocatalyst materials for water splitting. Chem Soc Rev, 2009, 38: 253–278
6 Kato H, Asakura K, Kudo A. Highly efficient water splitting into H_2 and O_2 over lanthanum-doped $NaTaO_3$ photocatalysts with high crystallinity and surface nanostructure. J Am Chem Soc, 2003, 125: 3082–3089
7 Liang S, Wu L, Bi J, et al. A novel solution-phase approach to nanocrystalline niobates: Selective syntheses of $Sr_{0.4}H_{1.2}Nb_2O_6{\cdot}H_2O$ nanopolyhedrons and $SrNb_2O_6$ nanorods photocatalysts. Chem Commun, 2010, 46: 1446–1448
8 Liang S, Shen L, Zhu J, et al. Morphology-controlled synthesis and efficient photocatalytic performances of a new promising photocatalyst $Sr_{0.25}H_{1.5}Ta_2O_6{\cdot}H_2O$. RSC Adv, 2011, 1: 458–467
9 Liang S, Wang X, Chen Y, et al. $Sr_{0.4}H_{1.2}Nb_2O_6{\cdot}H_2O$ nanopolyhedra: An efficient photocatalyst. Nanoscale, 2010, 2: 2262–2268